Insights into the regulation of cellular Mn2+ homeostasis via TMEM165

Dorothée Vicogne, Nicolas Beauval, Zoé Durin, Delphine Allorge, Kateryna Kondratska, Aurélien Haustrate, Natasha Prevarskaya, Vladimir Lupashin, Dominique Legrand, François Foulquier

Insights into the regulation of cellular Mn^{2+} homeostasis *via* TMEM165

Dorothée Vicogne[1], Nicolas Beauval[2], Zoé Durin[1], Delphine Allorge[2], Kateryna Kondratska[3,4], Aurélien Haustrate[3,4], Natasha Prevarskaya[3,4], Vladimir Lupashin[5], Dominique Legrand*[1], and François Foulquier*[1±]

[1]Univ. Lille, CNRS, UMR 8576 – UGSF - Unité de Glycobiologie Structurale et Fonctionnelle, F- 59000 Lille, France

[2]Univ. Lille, CHU Lille, Institut Pasteur de Lille, ULR 4483 - IMPECS - IMPact de l'Environnement Chimique sur la Santé humaine, F-59000 Lille, France

[3]Univ. Lille, INSERM U1003-PHYCEL-Physiology Cellulaire, F-59000 Lille, France

[4]Ion Channels Science and Therapeutics, Université de Lille, Villeneuve d'Ascq, France

[5]Department of Physiology and Biophysics, College of Medicine, University of Arkansas for Medical Sciences, Biomed 261-2, slot 505, 200 South Cedar St., Little Rock, AR, 72205, USA

Corresponding Author:

[±] François Foulquier (francois.foulquier@univ-lille.fr), Address: Univ. Lille, CNRS, UMR 8576 – UGSF - Unité de Glycobiologie Structurale et Fonctionnelle, F-59000 Lille, France.

Tel. + 33 3 20 43 44 30

Fax. +33 3 20 43 65 55

* These authors equally contributed to this work

Highlights

- Glycosylation defects in TMEM165 depleted cells arise from a lack of secretory pathway/organelles ~~Golgi~~ Mn homeostasis
- TMEM165 is a key protein in cellular Mn homeostasis
- Mn-detoxifying capacities of cells through the activity of SPCA1 depends on TMEM165 degradation

Abstract

Golgi cation homeostasis is known to be crucial for many cellular processes including vesicular fusion events, protein secretion, as well as for the activity of Golgi glycosyltransferases and glycosidases. TMEM165 was identified in 2012 as the first cation transporter related to human glycosylation diseases, namely the Congenital Disorders of Glycosylation (CDG). Interestingly, divalent manganese (Mn) supplementation has been shown to suppress the observed glycosylation defects in TMEM165-deficient cell lines, thus suggesting that TMEM165 is involved in cellular Mn homeostasis. This paper demonstrates that the origin of the Golgi glycosylation defects arises from impaired Golgi Mn homeostasis in TMEM165-depleted cells. We show that Mn supplementation fully rescues the Mn content in the secretory pathway/organelles of TMEM165-depleted cells and hence the glycosylation process. Strong cytosolic and organellar Mn accumulations can also be observed in TMEM165- and SPCA1-depleted cells upon incubation with increasing Mn concentrations, thus demonstrating the crucial involvement of these two proteins in cellular Mn homeostasis. Interestingly, our results show that the cellular Mn homeostasis maintenance in control cells is correlated with the presence of TMEM165 and that the Mn-detoxifying capacities of cells, through the activity of

SPCA1, rely on the Mn-induced degradation mechanism of TMEM165. Finally, this paper highlights that TMEM165 is essential in secretory pathway/organelles ~~Golgi~~ Mn homeostasis maintenance to ensure both Golgi glycosylation enzyme activities and cytosolic Mn detoxification.

1. Introduction

Divalent manganese (Mn^{2+}, Mn in the following) is a cofactor of oxidoreductases, transferases, hydrolases, lyases, isomerases and ligases necessary for many metabolic functions, energy production (plants) and anti-oxidant responses in living organisms (Tuschl et al., 2013)[1]. However, although playing crucial roles in many biological pathways, Mn belongs to the category of biometals whose mechanisms governing the cellular homeostasis are poorly understood, most especially in humans (Foulquier & Legrand, 2020)[2]. This is particularly true with regard to Mn homeostasis within the secretory pathway where this metal is required for the activity of key glycosyltransferases, such as the Golgi β-1,4-galactosyltransferase 1, involved in glycosylation processes (Ramakrishnan et al., 2004)[3]. Before the last ten years, only one protein dedicated to Mn transport could be identified within the secretory pathway, the Golgi protein SPCA1 (ATP2C1) belonging, like the endoplasmic reticulum (ER) pumps SERCA (SERCA1/ATP2A1 (muscle specific) and SERCA2/ATP2A2 (ubiquitous)), to the P-type Ca^{2+}-ATPase family (Palmgren & Nissen, 2011)[4]. While SERCA2 is primarily a Ca^{2+} ER importer, also able to transport Mn in certain conditions, SPCA1 may bind and transport Ca^{2+} and Mn with similar affinities (Chen et al., 2019)[5]. Actually, it was reported/hypothesized that the Mn transport function of SPCA1 better meets needs of metal detoxification from cytosol, as elevated Mn concentrations are toxic for the cells, than needs for maintaining Mn Golgi homeostasis (Leitch et al., 2011)[6]. In humans, SPCA1 deficiency causes the Hailey-Hailey disease (HHD), characterized by persistent blisters and erosions of the skin mainly due to impaired Ca^{2+} homeostasis in keratinocytes (Hu et al., 2000 ; Sudbrack et al., 2000)[7,8].

More recently, the discovery of patients with Congenital Disorders of Glycosylation (CDG) unveiled the existence of TMEM165 as a potential key player in Golgi Mn homeostasis (Foulquier et al., 2012 ; Zeevaert et al., 2012)[9,10]. Indeed, we reported that the strong glycosylation defects detected in TMEM165-CDG patients and TMEM165 KO cell lines,

affecting galactosylation in all glycosylation types (N- and O-glycosylations, glycolipids and glycosaminoglycans), may be fully rescued by Mn supplementation (Potelle et al., 2016 ; Morelle et al., 2017 ; Durin et al., 2022)[11–13,]. This important finding, together with i) the homology of TMEM165 with other members of the UPF0016 family transporting Mn and possibly also for some of them Ca^{2+} and/or H^{+} in plants (PAM71, CMT1, PML3-5 from *Arabidopsis thaliana*) (Schneider et al, 2016 ; Eisenhut et al., 2013 ; Hoecker et al., 2020)[14,15,16], cyanobacteria (SynPAM71/Mnx from Synechocystis) (Giandini et al., 2017)[17], and bacteria (MneA from *Vibrio cholerae*) (Brandenburg et al., 2017)[18], ii) the evidence that TMEM165 deficiency alters Golgi Mn homeostasis, as observed with the resistance of the Golgi Mn-sensitive GPP130 protein in TMEM165-deficient mammalian cells (Potelle et al., 2017)[19], iii) the sensitivity of TMEM165 itself to increased cytosolic Mn concentrations and its subsequent degradation in lysosomes (Potelle et al., 2017)[19] and iv) the measurement of the Mn transport activity *in Lactococcus lactis* of both a truncated form of TMEM165 and Gdt1p, the yeast ortholog of TMEM165 (Stribny et al., 2020)[20], strongly support the assertion that TMEM165 is a Mn Golgi importer playing a key role in regulating cellular Mn homeostasis.

From these findings, it thus appears that TMEM165 and SPCA1 are important, if not unique, into the regulation of the Golgi Mn homeostasis of this metal for detoxification purposes and/or metal supply to Golgi Mn-dependent glycosyltransferases. In support to this assertion, we recently evidenced a functional link between TMEM165 and SPCA1, by demonstrating that TMEM165 abundance in cells is directly dependent on the function of SPCA1 (Lebredonchel et al., 2019)[21]. In addition, in the pathological conditions of HHD (Hailey-Hailey Disease) where SPCA1 expression is impaired, the sensitivity of TMEM165 to elevated exogenous Mn concentrations has been found significantly increased (Roy et al., 2020)[22]. However, the conditions governing the Golgi Mn transport activity of TMEM165 and its interplay with SPCA1 in regulating Mn cellular homeostasis are unknown so far. This paper aims to study the

impact of a lack of TMEM165 on the capacity of cells to handle Mn contents within the cellular compartments, and to understand its role, together with SPCA1, in regulating secretory pathway/organelles Mn homeostasis and/or detoxification.

2. Methods

2.1 Antibodies and reagents

Anti-TMEM165 and anti-β-actin antibodies were purchased from Sigma-Aldrich (Burlington, MA, USA), anti-LAMP2 antibody from Santa Cruz Biotechnology (Dallas, TX, USA). Anti-SPCA1 antibodies were purchased from Sigma-Aldrich to be used in immunofluorescence staining (IF) and from Biotechne (Minneapolis, MN, USA) to be used in western-blotting (WB), anti-GM130 antibody was purchased from BD Biosciences (Franklin Lakes, NJ, USA). Polyclonal goat anti-rabbit or goat anti-mouse horseradish peroxydase-conjugated Igs were from Agilent Technologies (Santa Clara, CA, USA). Polyclonal goat anti-mouse or goat anti-rabbit conjugated with Alexa Fluor were purchased from Fisher Scientific (Waltham, MA, USA). Manganese (II) chloride tetrahydrate ($MnCl_2$) was from Riedel-de-Haën (Seelze, Germany). Digitonin was purchased from Fisher Scientific (Waltham, USA).

2.2 Cell culture and manganese treatment

TMEM165 and SPCA1 KO HeLa cells were generated as previously described in Vicogne et al., 2020 [23] and Hoffmann et al., 2017[24] respectively. Control and SPCA1 KO HeLa cells, as well as control and TMEM165 KO HeLa-GalT-GFP cells, were routinely grown in Dulbecco's Modified Eagle's Medium (DMEM) (Lonza, Basel, Switzerland) supplemented with 10% fetal bovine serum (PAN Biotech, Germany). Control and SPCA1 KO Hap1 cells were maintained in Iscove's Modified Dulbecco's Medium (IMDM) (Fisher Scientific, Waltham, USA) supplemented with 10% fetal bovine serum (PAN Biotech, Germany). All cell lines were maintained at 37°C in humidity-saturated 5% CO_2 atmosphere. When used, $MnCl_2$ was added for 16 hours at increasing concentrations, ranging from 1 to 400 µM.

2.3 Quantification of Mn by ICP-MS (Inductively Coupled Plasma-Mass Spectrometry)

2.3.1 Sample preparation

After $MnCl_2$ treatment in 12-well plates, cells were washed once with Hank's Balanced Salt Solution (HBSS) containing 1 mM of $MgCl_2$ and 2 mM of $CaCl_2$ and incubated with this solution for 2 hours at room temperature. Next, this solution was discarded and cells were washed three times with calcium- and magnesium-free HBSS ($HBSS^{-/-}$). Cells were permeabilized with $HBSS^{-/-}$ supplemented with digitonin (50 µM) for 1 min at room temperature to release cytosol content. This fraction was gently transferred into 1.5 mL tubes. Cells were immediately and quickly washed twice with $HBSS^{-/-}$ and these washings were added to the cytosolic fraction. To entirely lyse the cells, distilled water was added and cells were scrapped. Lysis extract was transferred into 1.5 mL tubes. This step was repeated once to assure maximal lysate recovery, added to the first extract and then sonicated for 1 min. Cytosolic fraction and lysate were stored at -20°C until further ICP-MS analysis.

2.3.2 Mn analysis

After separation, cytosolic and organelles samples were diluted 50 fold with 1.5% (w/v) nitric acid (RPE analytical grade 69.5%, Carlo Erba Reagents, Cornaredo, Italy) solution in ultrapure water (Purelab Flex, Veolia Water, Paris, France) also containing 0.1% (v/v) Triton™X-100 (Sigma-Aldrich, St Louis, MO, USA) and 0.2% (v/v) butan-1-ol (VWR chemicals, Radnor, PA, USA) The analysis was performed on an ICP-MS THERMO ICAP™ Qc ICP-MS (Thermo Scientific, Waltham, MA) using kinetic energy discrimination with helium and gallium as internal standard. The lower limit of quantification was 0.2 µg/L.

2.4 Western Blot analysis

Cells were scrapped in Dulbecco's Phosphate Buffer (DPBS, Lonza) and then centrifuged at 6000 rpm, 4°C for 10 min. Supernatant was discarded and cells were then resuspended in RIPA buffer [Tris/HCl 50 mM pH 7.9, NaCl 120 mM, NP40 0.5%, EDTA 1 mM, Na_3VO_4 1 mM, NaF 5 mM] supplemented with a protease cocktail inhibitor (Roche Diagnostics, Penzberg, Germany). Cell lysis was done by passing the cells several times through a syringe with a 26G

needle. Cells were centrifuged for 30 min, 4°C at 14 000 rpm. Protein concentration contained in the supernatant was estimated with the micro BCA Protein Assay Kit (Fisher Scientific, Waltham, USA) according to the manufacturer's instructions. Ten µg of total protein lysate were mixed with NuPAGE Lithium Dodecyl Sulfate (LDS) Sample Buffer (Fisher Scientific, Waltham, USA), pH 8.4, supplemented with 4% β-mercaptoethanol (Sigma-Aldrich, Saint Louis, USA). Samples were heated 10 min at 95°C (excepted for TMEM165 and SPCA1), then resolved by MOPS 4%-12% Bis-Tris gels (Fisher Scientific, Waltham, USA). After transfer with iBlot2 Dry Blotting System (Fisher Scientific, Waltham, USA), nitrocellulose membranes were blocked using TBS (Tris Buffer Saline) containing 0.05% Tween20 (TBS-T) and either 5% (w/v) non-fat dried milk (β-actin and LAMP2 antibodies) or 5% (w/v) bovine serum albumin (BSA) (TMEM165 and SPCA1 antibodies) for at least 1 h at room temperature (RT). Primary rabbit antibodies anti-TMEM165, mouse anti-SPCA1, mouse anti-β-actin, and mouse anti-LAMP2 were incubated overnight at 4°C in TBS-T and 5% (w/v) BSA or 5% (w/v) non-fat dried milk at respectively 1:1000, 1:4000, 1:10,000 and 1:3000 dilutions. After three TBS-T washes, membranes were then incubated with peroxidase-conjugated secondary goat anti-rabbit or goat anti-mouse antibodies (used at a dilution of 1:10,000 or 1:20,000 in blocking buffer) for 1 h at RT. After five TBS-T washes, blots were developed using enhanced chemiluminescence (West Pico Plus, ThermoScientific). The images were acquired using a CCD camera (Fusion Solo, Vilbert Lourmat).

2.5 Immunofluorescence staining

Cells were seeded on coverslips for 24h, washed twice in Dulbecco's Phosphate Buffer Saline (DPBS, Lonza) and fixed with 4% paraformaldehyde (PAF) in PBS (Phosphate Buffer Saline) pH 7.4 for 30 min at room temperature. Coverslips were then washed three times with PBS and cells were permeabilized with 0.5% Triton X-100 in PBS for 10 min before being washed three times with PBS. Coverslips were then incubated either for 2 h in BSA-Block (Candor-

Bioscience, Germany) (SPCA1 antibody) or for 1 h in blocking buffer (0.2% gelatin, 2% bovine serum albumin, 2% fetal bovine serum in PBS) (GM130 and TMEM165 antibodies) and then for 2 h with primary antibody diluted either at 1:100 (anti-SPCA1 and anti-GM130) or 1:300 (anti-TMEM165) in BSA-Block or blocking buffer. After 3 washings with PBS, cells were incubated for 1 h with Alexa Fluor 488-, or Alexa Fluor 568- conjugated secondary antibody (Fisher Scientific) diluted at 1:600 in BSA-Block or blocking buffer. After 3 washings with PBS, nuclei were labelled with DAPI 1:200 for 10 min and then mounted on glass slides with Mowiol. Fluorescence was detected by an inverted Zeiss LSM700 confocal microscope. Acquisitions were done using ZEN Pro2.1 Software (Zeiss, Oberkochen, Germany).

2.6 Statistical analysis

One-way ANOVA was used for statistical comparison of the differences. For each analysis, experiments have been done at least in triplicates. $p<0,05$ were considered as significant in experiments. For each graph, * : $p<0,05$; ** : $p<0,01$; *** : $p<0,001$."

3. Results

3.1 The observed glycosylation defect in TMEM165 KO cells results from a defect in membrane-bound organelles Mn homeostasis

Our previous work highlighted an unexpected functional link between TMEM165 and SPCA1 with a complete loss of TMEM165 observed in KO SPCA1 cells both by immunofluorescence and western blot (Lebredonchel et al., 2019 ; Potelle et al., 2017)[21,19], as confirmed in Figure 1 A,B. In contrast, the effect of a lack of TMEM165 on SPCA1 had never been investigated. For this, the abundance of SPCA1 was examined in KO TMEM165 cells by western blot and immunofluorescence (Fig. 1D, E). Compared to control cells, a slight decrease in SPCA1 (about 20%) is observed in KO TMEM165 cells (Fig. 1D, E). To confirm the involvement of TMEM165 in the observed SPCA1 decrease, wt-TMEM165 was transiently expressed in TMEM165 KO cells and the stability of SPCA1 was assessed by immunofluorescence. As shown in supplementary Figure 1, the transient expression of wt-TMEM165 rescues the abundance of SPCA1 in the Golgi. Moreover, and interestingly, a strong Golgi glycosylation defect was associated with the lack of TMEM165 (Fig. 1F), while absolutely no Golgi glycosylation abnormalities were observed in SPCA1 KO cells as assessed by the absence of LAMP2 electrophoretic mobility (Fig. 1C). We then hypothesized that this difference in Golgi glycosylation could arise from an impaired Golgi Mn homeostasis in TMEM165 KO cells, as previously suggested (Potelle et al., 2016 ; Morelle et al., 2017 ; Houdou et al., 2018 ; Vicogne et al., 2019 ; Khan et al., 2021)[11,12,25,23,26]. To tackle this fundamental point, Mn levels in cytosol versus intracellular compartments were assessed by using a well-known and robust methodology based on digitonin action that only permeabilizes, when used at low concentration (0.01-0.02% (w/v)), the plasma membrane (Niklas et al., 2011)[27]. The digitonin cell permeabilization protocol that will be used throughout the paper is depicted in supplementary Figure 2. This selective permeabilization therefore releases cytosolic solutes leaving the content

of intracellular compartments such as endoplasmic reticulum (ER), Golgi apparatus, mitochondria, endosomes and nucleus unchanged. Via this methodology, the Mn amounts in the cytosol versus intracellular compartments can then be quantified using inductively-coupled plasma mass spectrometry (ICP-MS). This was applied to TMEM165 and SPCA1 KO cells.

At the steady state (no exogenous Mn added), the cytosolic Mn content was found similar in TMEM165 KO, SPCA1 KO and control HeLa cells (Fig. 2A). Regarding the membrane-bound organelle fraction, a 10-fold decrease in Mn concentration was observed in TMEM165 KO cells compared to SPCA1 KO and control HeLa cells (Fig. 2A). Given this astonishing absence of Mn accumulation in SPCA1 KO cells, which lacks both SPCA1 and TMEM165 (Fig. 1A, B), the same experiment was performed in another cellular background, namely SPCA1 KO Hap1 cells (Supplementary Figure 3). In SPCA1 KO Hap1 cells, 5.8- and 1.4-fold Mn increases were observed in the cytosolic and membrane-bound organelles fractions, respectively, as compared to control cells, highlighting the establishment in HeLa cells of compensatory mechanisms to maintain their Mn homeostasis.

We then focused on the very low Mn concentration observed in the membrane-bound organelle fraction of TMEM165 KO cells asking whether this decreased Mn amount would account for the observed massive Golgi glycosylation defects in TMEM165 KO cells. To tackle this question, TMEM165 KO cells were next treated with 1 μM Mn for 16 h, a condition that is known to fully suppress the glycosylation defects (Fig. 2B), and Mn quantification was re-performed. In such conditions, 3.5 and 4.8-fold increases in Mn concentration can be observed in membrane-bound organelles of control and TMEM165 KO cells, respectively (Fig. 2A). Furthermore, it is interesting to note that the Mn amount observed in TMEM165 KO cells treated with 1 μM Mn is close to the one observed in control cells without Mn treatment. In parallel, the same treatment was applied to SPCA1 KO cells. Interestingly, whereas the control cells significantly accumulated Mn in their membrane-bound organelles, with no or little Mn

accumulation in their cytosol, the SPCA1 KO cells exhibited a drastic accumulation of Mn in both cytosolic and membrane-bound organelle compartments, of the order of 4.2 and 6.6-fold respectively, as compared to control cells. This result demonstrates a clear defect in cellular Mn homeostasis maintenance in SPCA1 KO cells when only 1 μM $MnCl_2$ was applied. Altogether these results unravel that the observed Golgi glycosylation defect in TMEM165 KO cells originates from a lack of Mn in membrane-bound organelles, most likely in the Golgi apparatus given the Golgi subcellular localization of TMEM165.

3.2 Both TMEM165 and SPCA1 are crucial in maintaining cytosolic and membrane-bound organelles Mn homeostasis

The previous results strongly suggest a Mn transport mechanism from the cytosol to the Golgi lumen *via* TMEM165. If correct, TMEM165 deficiency should lead to an increase of the cytosolic Mn content upon increasing Mn supplementation. To assess this hypothesis, control, TMEM165 and SPCA1 KO HeLa cells were first incubated with increasing moderate Mn concentrations (0 to 50 μM) for 16 h and the digitonin cell permeabilization methodology was applied to quantify the cytosolic and membrane-bound organelle Mn contents. As depicted in Figure 3 and supplementary Figure 4 for statistical comparisons, no cytosolic Mn accumulation was observed in control cells, in sharp contrast with the marked increase of Mn content observed in both TMEM165 and SPCA1 KO cells incubated with increasing $MnCl_2$ concentrations from 2.5 to 50 μM. In particular, upon incubation with 25 μM $MnCl_2$, the TMEM165 KO cells exhibited an 8.9-fold higher cytosolic Mn content than the one observed in control cells. Although the slope of cytosolic Mn accumulation is similar between TMEM165 and SPCA1 KO cells, a two-fold accumulation of Mn is seen in SPCA1 KO cells compared to TMEM165 KO cells. Since SPCA1 KO cells lack both SPCA1 and TMEM165, it may thus be deduced that both proteins participate in the efflux of Mn from the cytosol.

Regarding the membrane-bound organelle fraction, Mn concentration increased in all three cell lines but with completely different orders of magnitude (Fig. 3). In control cells, the Mn concentration raised slightly upon 1 µM Mn incubation then remained stable for increasing Mn concentrations, thus demonstrating a tight Mn homeostasis regulation of membrane-bound organelles. This contrasts with the results obtained in both TMEM165 and SPCA1 KO cells where a marked Mn concentration increase is seen (2.3 and 8.1-fold for TMEM165 KO and SPCA1 KO cells, respectively, as compared to control cells).

We then wondered what would happen for higher $MnCl_2$ concentrations (100 to 400 µM for 16 h). As shown in Figure 4A, whereas the control cells kept their cytosolic Mn content low till 100 µM $MnCl_2$, a 3.2-fold increase was achieved at 200 µM $MnCl_2$ and, surprisingly, a level similar to that observed in TMEM165 KO cells was reached at 400 µM $MnCl_2$ (36.5-fold increase). This obviously leads to repercussions on the membrane-bound organelle Mn content at 400 µM $MnCl_2$, most especially that of SPCA1 KO cells lacking both SPCA1 and TMEM165 (Fig. 4A). Altogether our results indicate that, in control cells, TMEM165 is essential in regulating the cytosolic Mn homeostasis till 200 µM of exogenous $MnCl_2$, and that above that concentration (400 µM $MnCl_2$ in our experiment), it does not seem longer functional. In order to explain this phenomenon, the stability of TMEM165 was followed. As shown in Figure 4B, the stability of TMEM165 in control cells was found markedly decreased from 100 to 400 µM $MnCl_2$ with the presence of lighter molecular weight protein bands (down to 25 kDa) likely corresponding to degradation forms of TMEM165. This confirms our previous results demonstrating the Mn-induced degradation of TMEM165 upon $MnCl_2$ treatment and its blocking by lysosomal inhibitors (Potelle et al., 2017)[19]. Altogether these findings highlight a strong correlation between the markedly-increased accumulation of cytosolic Mn in control cells and the observed Mn-induced degradation of TMEM165.

These intriguing results prompted us to similarly evaluate the cellular Mn content in SPAC1 KO cells deficient for both SPCA1 and TMEM165. Therefore, SPCA1 KO cells were treated with $MnCl_2$ concentrations from 100 to 400 µM for 16 h and the same methodology was applied. Upon 100 µM $MnCl_2$ incubation, the SPCA1 KO cells exhibited a 16-fold higher Mn cytosolic content than the one observed in control cells but similar to that observed in TMEM165 KO cells (14.2-fold increase) (Fig. 4A). Intriguingly, the corresponding Mn amounts found in the membrane-bound organelles of SPCA1 KO cells were 11.3-fold higher than in control cells, and 3.3-fold higher than in TMEM165 KO cells. In conclusion, although no difference can be observed between TMEM165 KO and SPCA1 KO cells with regard to Mn accumulation in their cytosol, a marked difference resides in their membrane-bound organelle Mn content, about twice higher in SPCA1 KO cells than in TMEM165 KO cells.

3.3 SPCA1 activity is affected in TMEM165 KO cells

This observed accumulation of Mn in the cytosol but also in membrane-bound organelles of control, TMEM165 and SPCA1 KO cells upon 400 µM $MnCl_2$ treatment led us to investigate the Mn detoxification capacities of these cells. According to the literature, one way to cope with cytosolic Mn excess involves the activity of SPCA1 in a so-called detoxification pathway (Leitch et al., 2011)[6]. For assessing the detoxification capacities and for comparisons, the cells were treated with different $MnCl_2$ concentrations to reach about the same Mn contents whether in cytosol or in membrane-bound organelles. To this end, control and TMEM165 KO cells were incubated with 400 µM $MnCl_2$ and SPCA1 KO cells with 100 µM $MnCl_2$. Cells were then washed and incubated in a free Mn medium for 3 and 6 h and subjected to our cell permeabilization methodology to evaluate and compare the kinetic of Mn detoxification in the cytosol and membrane-bound organelles. As shown in Figure 5, the cytosolic Mn detoxification of control cells was very efficient as the initial cytosolic Mn pool decreased by 79 and 93% after 3 and 6h, respectively. In SPCA1 KO cells, in contrast, the cytosolic Mn detoxification

occurred at a much slower rate as the initial cytosolic pool decreases by only 30 and 54% after 3 and 6 h, respectively. Since the difference between the two curves is supposed to reflect the activity of SPCA1 in cytosolic Mn detoxification, it may be assumed that in control cells, about 50% of the observed Mn detoxification is due to the activity of SPCA1. It is also important to note that, in this set of experiments, the contribution of TMEM165 is negligible as found absent in both control (incubated with 400 μM $MnCl_2$) and SPCA1 KO cells. Regarding TMEM165 KO cells, the result is close to the one observed in SPCA1 KO cells, with 41 and 78% cytosolic Mn content decreases after 3 and 6 h, respectively. Since TMEM165 is absent in 400 μM $MnCl_2$-treated control cells as well as in TMEM165 KO cells, these results highly suggest that SPCA1's activity in detoxifying cytosolic Mn is likely altered in TMEM165 KO cells.

Concerning the Mn detoxification associated with membrane-bound organelles, our results are similar to those obtained above. A much slower detoxification is seen in SPCA1 KO cells compared to control and TMEM165 KO cells. 38 and 54% decreases are observed for SPCA1 KO cells after 3 and 6h, respectively, compared to 57% and 70% for TMEM165 KO cells and 69% and 85% for control cells. This suggests that only about 50% of the accumulating Mn in SPCA1 KO cells is mobilizable for secretion instead of 85% for control cells.

4. Discussion

TMEM165 was described in 2012 as a new gene related to human glycosylation diseases, namely Congenital Disorders of Glycosylation (CDG) (Foulquier et al. 2012)[9]. Since then, many achievements were done to decipher the function of TMEM165 in the etiology of the glycosylation deficiency. Our results highlighted that the singularity of TMEM165 deficiency lies in the general observed glycosylation defects, as synthesis of N- and O-linked glycans, glycosphingolipids and glycosaminoglycans (GAGs) was shown to be altered (Foulquier et al., 2012 ; Schulte Althoff et al., 2015 ; Bammens et al., 2015 ; Morelle et al., 2017 ; Khan et al., 2021, Durin et al., 2022)[9,28,29,12,26]. Although TMEM165 deficiency can affect most of the Golgi glycosylation reactions, the galactosylation reaction was found severely altered in all the aforementioned different glycosylation types. As galactosylation is fundamental in lactose synthesis, we postulated in 2012 that TMEM165 should be crucial in such synthesis. This was demonstrated in 2014 and 2019 by Reinhardt and Snyder. They both observed strong milk quality defects with lower lactose, calcium and manganese levels in Tmem165 knockout mice (Foulquier et al., 2012, Reinhardt et al., 2014, Snyder et al., 2019) [9,30,31]. These results led to a model where TMEM165 would import both cytosolic Mn2+ and Ca2+ to the Golgi in exchange for H+ as over acidification of the Golgi apparatus and acidic compartments in TMEM165 depleted cells was evidenced (Wang et al., 2020, Demaegd et al., 2013) [32,33]. The function of TMEM165 in regulating cellular Mn homeostasis was figured out much later from many observations, and particularly from the fact that all the observed TMEM165-associated glycosylation defects could fully be suppressed by tiny amounts of exogenous $MnCl_2$ (Potelle et al., 2016 ; Morelle et al., 2017 ; Houdou et al., 2018 ; Vicogne et al., 2019, Durin et al., 2022)[11,12,25,23]. This observation has been the keystone to postulate that TMEM165 could be a Mn transporter crucial to provide Mn into the Golgi, itself conducive to the activities of the Mn-dependent glycosylation enzymes present in that organelle. Together with mitochondria and

nucleus, Golgi is known to constitute an important membrane-bound organelle for Mn storage (Das et al., 2019 ; Gavin et al., 1999 ; Kalia et al., 2008)[34,35,36]. Many pumps and transporters are involved in regulating Mn homeostasis along the secretory pathway, in post-Golgi vesicles and also at the plasma membrane. For example, human Zn transporters such as SLC39A8, SLC30A10 and SLC39A14 have been shown to contribute to cellular Mn homeostasis but most of these transporters are non-specific and can transport other cationic biometals (Bosomworth et al., 2012, Taylor et al., 2005, Nebert & Liu., 2019, Girijashanker et al., 2008, Guthrie et al., 2014, Liu et al., 2008)[37–41].At the steady state, the observed Mn concentration in one specific compartment not only results from the combined activities of the different transporters and pumps but also of the concentration of other metals. Although crucial in our understanding, the impact of a lack of TMEM165 on cellular Mn homeostasis had never been investigated, primarily caused by the absence of either truly specific and/or sensitive Mn sensors or practical and/or cost-effective biophysical methods, unlike radioactive trace assays or the synchrotron X-ray fluorescence nanoimaging (Carmona et al., 2010 ; Das et al., 2019)[42,43]. The Ca^{2+} fluorescent indicator Fura-2 AM is the most used Mn sensor as it can measure intracellular Mn by quenching, but only in relative amounts (Kwakye et al., 2011)[44]. Furthermore, Fura-2 AM can only cross the plasma membrane, not the membranes of organelles. Interestingly, a new method, called MESMER (Manganese-Extracting Small Molecule Estimation Route) was recently developed (Horning et al., 2020)[45]. Based on Mn-induced Fura-2 quenching, it uses a selective Mn ionophore called MESM (Manganese-Extracting Small Molecule) enabling non-lethal quantification of cellular Mn. However, it is unclear whether MESM crosses intracellular membranes (Horning et al., 2020)[45] and MESMER thus does not constitute a suitable method. In this paper, we used a digitonin cell permeabilization based approach, coupled to ICP-MS analysis, to investigate and quantify the differential amounts of Mn in the cytosol and membrane-bound organelles of control, SPCA1 and TMEM165 KO cells.

We first show that, when cells were not supplemented with Mn, the Mn amount in membrane-bound organelles was 4-fold decreased in TMEM165 KO cells compared to control or SPCA1 KO cells. Given the Golgi localization of TMEM165, it may be assumed that the observed Mn decrease most likely affects the Golgi compartment then explaining the origin of the observed glycosylation deficiencies, while demonstrating a major role of TMEM165 in the maintenance of Golgi Mn homeostasis. Interestingly, the supplementation of the culture medium with 1 µM $MnCl_2$ was sufficient to restore the Mn level associated to membrane-bound organelles to the one initially seen in control cells in absence of exogenous Mn. This result perfectly correlates with the reappearance of fully-glycosylated LAMP2 protein forms observed following supplementation of the culture medium with 1 µM $MnCl_2$, and hence strongly supports a functional role of TMEM165 in the maintenance of the Mn homeostasis in membrane-bound organelles, most likely in the Golgi. It is important to note that the same treatment in SPCA1 KO cells, which lack both SPCA1 and TMEM165, leads to a sharp increase of Mn in both cytosol and membrane-bound organelles, somehow demonstrating the fundamental importance of SPCA1, in addition to TMEM165, in regulating cellular Mn homeostasis upon mild Mn supplementation.

The question on how Mn could reach the Golgi lumen and rescue the glycosylation in absence of TMEM165 particularly caught our attention and was tackled in our previous study (Houdou et al., 2018)[25]. We indeed revealed that the Mn-induced N-glycosylation rescue in TMEM165 KO HEK cells is dependent on the Mn pumping activity of ER SERCA pumps (Figure 6). Once pumped in the ER, we can reasonably hypothesized that this Mn is redistributed into the Golgi apparatus presumably *via* vesicular trafficking (Houdou et al., 2018)[25]. This concept is fully in line with the work of Kaufman *et al.* (Kaufman et al., 1994)[46] arguing that the requirement for Mn for oligosaccharide addition within the secretory pathway is sensitive to thapsigargin, an inhibitor of SERCA pumps.

Another very important result is the crucial involvement of both TMEM165 and SPCA1 in the regulation of the cytosolic and membrane-bound organelle Mn homeostasis, as increasing exogenous $MnCl_2$ concentrations led to a markedly increased amount of Mn in the cytosol and membrane-bound organelles of TMEM165 KO cells and foremost SPCA1 KO cells lacking both SPCA1 and TMEM165. Indeed, while control cells can fully regulate their cellular Mn homeostasis upon Mn supplementation up to 100 µM, the lack of either TMEM165 or both SPCA1 and TMEM165 leads to a sharp accumulation of Mn in both cytosol and membrane-bound organelles. Whatever the extracellular Mn concentration applied, the observed Mn accumulation was always found higher in SPCA1 KO cells than in TMEM165 KO cells that is somehow logical if we consider the lack of TMEM165 in SPCA1 KO cells. This demonstrates that TMEM165 and SPCA1 work together in preventing cytosolic Mn accumulation. How then to explain the observed sharp accumulation of Mn in membrane-bound organelles in SPCA1 and TMEM165 KO cells? Analyzing the control cells enables us to see a much higher Mn accumulation in membrane-bound organelles than in cytosol, thus suggesting that membrane-bound organelles may play the role of reservoir to keep the cytosolic Mn content low. Therefore, we can hypothesize that the observed cytosolic Mn accumulation in SPCA1 and TMEM165 KO cells upon supplementation with increasing extracellular Mn concentrations leads to the fueling of different reservoirs within these cells, then explaining the observed Mn increase in membrane-bound organelles. The pulse-chase methodology interestingly shows that, in SPCA1 KO cells, 50% of the accumulating Mn cannot be extruded from the cell, going to 30% for TMEM165 KO cells and only 10% for control cells. This thus suggests that in SPCA1 KO cells, which also lack TMEM165, most of the accumulating Mn redistributes in other subcellular compartments than those from the secretory pathway, likely mitochondria and/ or nucleus.

Another last very surprising result is that control cells exhibit Mn contents similar to that of TMEM165-deficient cells upon incubation with $MnCl_2$ concentrations reaching 400 µM.

Actually, our previous work showed that for similar $MnCl_2$ concentrations, TMEM165 was targeted to lysosomes for degradation (Potelle et al., 2017)[19]. Here, we intriguingly show that the exogenous Mn-induced instability of TMEM165 correlates with the markedly-increased amounts of Mn in control cells, in both cytosol and membrane-bound organelles. This finding raises a number of questions about the functionality of SPCA1 upon 400 µM $MnCl_2$ treatment, whether in control or TMEM165 KO cells. In human cells, it is indeed well known that one way to cope with cytosolic Mn excess involves SPCA1, an ATPase pump able to import Mn into the Golgi lumen for its removal (Leitch et al., 2011)[6]. Two main hypotheses can be raised to explain the observed Mn accumulation in control cells upon 400 µM $MnCl_2$: (i) TMEM165 itself is involved in the detoxification of cytosolic Mn excess upon $MnCl_2$ exposure and/or (ii) the absence of TMEM165 impacts SPCA1's function. In support to the second hypothesis, our previous works highlighted a functional link between TMEM165 and SPCA1 (Lebredonchel et al., 2019 ; Roy et al., 2020)[21,22]. We indeed demonstrated that the protein expression level and Golgi subcellular localization of TMEM165 are dependent on SPCA1's function to import cytosolic Mn into the Golgi lumen. A lack of SPCA1 results in cytosolic Mn accumulation, itself causing a specific targeting of TMEM165 to lysosomes for degradation. This result somehow argues that SPCA1 is active in detoxifying Mn in control cells, and that the sole Mn pumping activity of TMEM165, if any, is not sufficient to decrease the accumulating cytosolic Mn. This reinforces the hypothesis that the absence of TMEM165 could impact SPCA1's function. To tackle this point, we evaluated the kinetic of cytosolic Mn detoxification in control cells, TMEM165 KO and SPCA1 KO cells. Whereas the cytosolic Mn decreased rapidly in control cells, TMEM165 KO cells exhibited a slower rate, even though faster than the one observed in SPCA1 KO cells. Although SPCA1 is slightly decreased in TMEM165 KO cells, this difference in the slopes suggests that the function of SPCA1 may be altered in absence of TMEM165. It is also important to note that a strong difference is observed in cytosolic Mn

decrease between control and TMEM165 KO cells upon $MnCl_2$ exposure, although TMEM165 is absent in control cells at these exogenous Mn concentrations. The difference could correspond to the impact of the Mn-induced degradation of TMEM165 caused by SPCA1 activation. Taken as a whole, these results suggest that the degradation of TMEM165 could be a prerequisite in activating SPCA1 in Mn detoxification. For low extracellular Mn concentrations, it is possible that TMEM165 plays the dual function of maintaining the Golgi Mn homeostasis, necessary for Mn-dependent processes such as glycosylation, as well as detoxifying the cytosol from Mn accumulation. For higher extracellular Mn concentrations, we can imagine that SPCA1 is turned on to speed up the detoxification and this requires TMEM165 degradation (Figure 6). In absence of TMEM165, SPCA1 could simply be less active in detoxifying Mn as pumping Ca2+. This hypothesis is perfectly in line with our previous results on GPP130, another Mn-sensitive protein (Masuda et al., 2013)[47]. Initially, it has been demonstrated by us and others that the Mn-induced GPP130 degradation is linked to the functionality of SPCA1 in pumping Mn (Mukhopadhyay & Linstedt, 2011 ; Potelle et al., 2016 ; Lebredonchel et al., 2019)[48,11,21]. In TMEM165 KO cells, we always observed that the Mn-induced degradation of GPP130 upon $MnCl_2$ treatment was strongly altered bringing us to postulate that TMEM165 could contribute to import Mn from the cytosol to the Golgi lumen (Potelle et al., 2016)[11]. In the light of our results, it could well rather be due to a lack of SPCA1 activity in TMEM165 KO cells. It is also important to note that the estimated cytosolic Mn concentration of HeLa cells without Mn supplementation, deduced from our ICP-MS measurements and in accordance with estimates of other authors on brain cells (Bowman & Ashner, 2014 ; Horning et al., 2020)[45,49] , is close to 10 µM. Hence, in comparison to Ca^{2+} whose cytosolic concentration is around 0.1 µM, the cytosol contains about 100 times more Mn^{2+} than Ca^{2+}! Given the similar Km for Mn^{2+} and Ca^{2+} regarding SPCA1, in the submicromolar range (Chen et al., 2019 ; van Baelen et al., 2001)[5,50] suggests that at low ion

availability the relative Ca^{2+} and Mn^{2+}concentrations will determine which ion will be transported by SPCA1. One can asks how SPCA1 can then efficiently transports Ca^{2+} in the Golgi compartment. This could only be envisaged by a very tight regulation of SPCA1 likely via TMEM165.

Altogether our results suggest that TMEM165 would act both in cytosolic Mn accumulation and in maintaining secretory pathway/organelles Mn concentration for Golgi glycosylation enzymes activities. This would allow SPCA1 to maintain TGN Ca homeostasis which is critical for many Golgi functions. For exogenous Mn concentration above 200 µM, TMEM165 would be degraded to "turn on" SPCA1 in the Mn detoxification pathway (Fig. 6).

In conclusion, this paper for the first time brings the evidence on the crucial role of TMEM165 in regulating both cytosolic and membrane-bound organelle Mn homeostasis. It also highlights the functional interplay between TMEM165 and SPCA1 in preventing cytosolic Mn accumulation and eventually, we proved that the Golgi glycosylation defect observed in TMEM165 KO cells correlates with the decrease of Mn in secretory pathway/ organelles.

CRediT authorship contribution statement

Funding acquisition: F.F. Investigation: D.V, N.B, Z.D, K.K, A.H, N.P, V.L, D.L, F.F. Supervision D.L and F.F. Validation: D.V, N.B, D.A, Z.D, K.K. Writing - review and editing: D.V, V.L, D.L and F.F.

All authors commented on previous versions of the manuscript. All authors read and approved the final manuscript.

Funding

This work was supported by the ANR ENIGMnCA (ANR-21-CE14-0049-01) to F.F and by the "Centre National de la Recherche Scientifique" (CNRS).

Declaration of competing interest

The authors declare no conflict of interest and all authors were involved in the decision to publish and reviewed the article before submission

Data availability

Data will be made available on request.

Acknowledgments

We deeply thank Hans-Heinrich Hoffmann and Charles M Rice for kindly providing the SPCA1 knockout cells. We acknowledge the access to the BICeL-UMS2014-US41 platform. The authors also warmly thank the technical team of the Toxicology Laboratory of the Lille University Hospital for the manganese analysis.

References

1. Tuschl, K., Mills, P. B. & Clayton, P. T. Manganese and the brain. *Int Rev Neurobiol* **110**, 277–312 (2013).

2. Foulquier, F. & Legrand, D. Biometals and glycosylation in humans: Congenital disorders of glycosylation shed lights into the crucial role of Golgi manganese homeostasis. *Biochim Biophys Acta Gen Subj* **1864**, 129674 (2020).

3. Ramakrishnan, B., Boeggeman, E., Ramasamy, V. & Qasba, P. K. Structure and catalytic cycle of beta-1,4-galactosyltransferase. *Curr. Opin. Struct. Biol.* **14**, 593–600 (2004).

4. Palmgren, M. G. & Nissen, P. P-type ATPases. *Annu Rev Biophys* **40**, 243–266 (2011).

5. Chen, J. *et al.* An N-terminal Ca2+-binding motif regulates the secretory pathway Ca2+/Mn2+-transport ATPase SPCA1. *J. Biol. Chem.* **294**, 7878–7891 (2019).

6. Leitch, S. *et al.* Vesicular distribution of Secretory Pathway Ca2+-ATPase isoform 1 and a role in manganese detoxification in liver-derived polarized cells. *Biometals* **24**, 159–170 (2011).

7. Hu, Z. *et al.* Mutations in ATP2C1, encoding a calcium pump, cause Hailey-Hailey disease. *Nat Genet* **24**, 61–65 (2000).

8. Sudbrak, R. *et al.* Hailey-Hailey disease is caused by mutations in ATP2C1 encoding a novel Ca(2+) pump. *Hum. Mol. Genet.* **9**, 1131–1140 (2000).

9. Foulquier, F. *et al.* TMEM165 Deficiency Causes a Congenital Disorder of Glycosylation. *The American Journal of Human Genetics* **91**, 15–26 (2012).

10. Zeevaert, R. *et al.* Bone Dysplasia as a Key Feature in Three Patients with a Novel Congenital Disorder of Glycosylation (CDG) Type II Due to a Deep Intronic Splice Mutation in TMEM165. in *JIMD Reports - Case and Research Reports, 2012/5* (eds. Zschocke, J., Gibson, K. M., Brown, G., Morava, E. & Peters, V.) vol. 8 145–152 (Springer Berlin Heidelberg, 2012).

11. Potelle, S. *et al.* Glycosylation abnormalities in Gdt1p/TMEM165 deficient cells result from a defect in Golgi manganese homeostasis. *Hum Mol Genet* **25**, 1489–1500 (2016).

12. Morelle, W. *et al.* Galactose Supplementation in Patients With TMEM165-CDG Rescues the Glycosylation Defects. *J Clin Endocrinol Metab* **102**, 1375–1386 (2017).

13. Durin, Z. *et al.* Differential Effects of D-Galactose Supplementation on Golgi Glycosylation Defects in TMEM165 Deficiency. *Front Cell Dev Biol* **10**, 903953 (2022).

14. Schneider, A. *et al.* The Evolutionarily Conserved Protein PHOTOSYNTHESIS AFFECTED MUTANT71 Is Required for Efficient Manganese Uptake at the Thylakoid Membrane in Arabidopsis. *Plant Cell* **28**, 892–910 (2016).

15. Eisenhut, M. *et al.* The Plastid Envelope CHLOROPLAST MANGANESE TRANSPORTER1 Is Essential for Manganese Homeostasis in Arabidopsis. *Mol Plant* **11**, 955–969 (2018).

16. Hoecker, N., Honke, A., Frey, K., Leister, D. & Schneider, A. Homologous Proteins of the Manganese Transporter PAM71 Are Localized in the Golgi Apparatus and Endoplasmic Reticulum. *Plants (Basel)* **9**, (2020).

17. Gandini, C., Schmidt, S. B., Husted, S., Schneider, A. & Leister, D. The transporter SynPAM71 is located in the plasma membrane and thylakoids, and mediates manganese tolerance in Synechocystis PCC6803. *New Phytol* **215**, 256–268 (2017).

18. Brandenburg, F. *et al.* The Synechocystis Manganese Exporter Mnx Is Essential for Manganese Homeostasis in Cyanobacteria. *Plant Physiol.* **173**, 1798–1810 (2017).

19. Potelle, S. *et al.* Manganese-induced turnover of TMEM165. *Biochemical Journal* **474**, 1481–1493 (2017).

20. Stribny, J., Thines, L., Deschamps, A., Goffin, P. & Morsomme, P. The human Golgi protein TMEM165 transports calcium and manganese in yeast and bacterial cells. *J. Biol. Chem.* **295**, 3865–3874 (2020).

21. Lebredonchel, E. *et al.* Investigating the functional link between TMEM165 and SPCA1. *Biochem. J.* **476**, 3281–3293 (2019).

22. Roy, A.-S. *et al.* SPCA1 governs the stability of TMEM165 in Hailey-Hailey disease. *Biochimie* **174**, 159–170 (2020).

23. Vicogne, D. *et al.* Fetal Bovine Serum impacts the observed N-glycosylation defects in TMEM165 KO HEK cells. *J. Inherit. Metab. Dis.* **43**, 357–366 (2019).

24. Hoffmann, H.-H. *et al.* Diverse viruses require the calcium transporter SPCA1 for maturation and spread. *Cell Host Microbe* **22**, 460-470.e5 (2017).

25. Houdou, M. *et al.* Involvement of thapsigargin and cyclopiazonic acid-sensitive pumps in the rescue of TMEM165-associated glycosylation defects by Mn2. *FASEB J.* **33**, 2669–2679 (2018).

26. Khan, S., Sbeity, M., Foulquier, F., Barré, L. & Ouzzine, M. TMEM165 a new player in proteoglycan synthesis: loss of TMEM165 impairs elongation of chondroitin- and heparan-sulfate glycosaminoglycan chains of proteoglycans and triggers early chondrocyte differentiation and hypertrophy. *Cell Death Dis* **13**, 1–14 (2021).

27. Niklas, J., Melnyk, A., Yuan, Y. & Heinzle, E. Selective permeabilization for the high-throughput measurement of compartmented enzyme activities in mammalian cells. *Anal Biochem* **416**, 218–227 (2011).

28. Schulte Althoff, S. *et al.* TMEM165 Deficiency: Postnatal Changes in Glycosylation. *JIMD Rep* **26**, 21–29 (2015).

29. Bammens, R. *et al.* Abnormal cartilage development and altered N-glycosylation in Tmem165-deficient zebrafish mirrors the phenotypes associated with TMEM165-CDG. *Glycobiology* **25**, 669–682 (2015).

30. Reinhardt, T. A., Lippolis, J. D. & Sacco, R. E. The Ca(2+)/H(+) antiporter TMEM165 expression, localization in the developing, lactating and involuting mammary gland parallels the secretory pathway Ca(2+) ATPase (SPCA1). *Biochem Biophys Res Commun* **445**, 417–421 (2014).

31. Snyder, N. A., Palmer, M. V., Reinhardt, T. A. & Cunningham, K. W. Milk biosynthesis requires the Golgi cation exchanger TMEM165. *J Biol Chem* **294**, 3181–3191 (2019).

32. Wang, H. *et al.* In Situ Fluorescent and Photoacoustic Imaging of Golgi pH to Elucidate the Function of Transmembrane Protein 165. *Anal Chem* **92**, 3103–3110 (2020).

33. Demaegd, D. *et al.* Newly characterized Golgi-localized family of proteins is involved in calcium and pH homeostasis in yeast and human cells. *Proc Natl Acad Sci U S A* **110**, 6859–6864 (2013).

34. Das, S. *et al.* Manganese Mapping Using a Fluorescent Mn2+ Sensor and Nanosynchrotron X-ray Fluorescence Reveals the Role of the Golgi Apparatus as a Manganese Storage Site. *Inorg Chem* **58**, 13724–13732 (2019).

35. Gavin, C. E., Gunter, K. K. & Gunter, T. E. Manganese and calcium transport in mitochondria: implications for manganese toxicity. *Neurotoxicology* **20**, 445–453 (1999).

36. Kalia, K., Jiang, W. & Zheng, W. Manganese accumulates primarily in nuclei of cultured brain cells. *Neurotoxicology* **29**, 466–470 (2008).

37. Bosomworth, H. J., Thornton, J. K., Coneyworth, L. J., Ford, D. & Valentine, R. A. Efflux function, tissue-specific expression and intracellular trafficking of the Zn transporter ZnT10 indicate roles in adult Zn homeostasis. *Metallomics* **4**, 771–779 (2012).

38. Taylor, K. M., Morgan, H. E., Johnson, A. & Nicholson, R. I. Structure-function analysis of a novel member of the LIV-1 subfamily of zinc transporters, ZIP14. *FEBS Lett* **579**, 427–432 (2005).

39. Nebert, D. W. & Liu, Z. SLC39A8 gene encoding a metal ion transporter: discovery and bench to bedside. *Hum Genomics* **13**, 51 (2019).

40. Girijashanker, K. *et al.* Slc39a14 gene encodes ZIP14, a metal/bicarbonate symporter: similarities to the ZIP8 transporter. *Mol Pharmacol* **73**, 1413–1423 (2008).

41. Liu, Z. *et al.* Cd2+ versus Zn2+ uptake by the ZIP8 HCO3--dependent symporter: kinetics, electrogenicity and trafficking. *Biochem Biophys Res Commun* **365**, 814–820 (2008).

42. Carmona, A. *et al.* Manganese accumulates within golgi apparatus in dopaminergic cells as revealed by synchrotron X-ray fluorescence nanoimaging. *ACS Chem Neurosci* **1**, 194–203 (2010).

43. Das, S. *et al.* Manganese Mapping Using a Fluorescent Mn2+ Sensor and Nanosynchrotron X-ray Fluorescence Reveals the Role of the Golgi Apparatus as a Manganese Storage Site. *Inorg Chem* **58**, 13724–13732 (2019).

44. Kwakye, G. F., Li, D., Kabobel, O. A. & Bowman, A. B. Cellular fura-2 manganese extraction assay (CFMEA). *Curr Protoc Toxicol* **12**, Unit12.18 (2011).

45. Horning, K. J. *et al.* Identification of a selective manganese ionophore that enables nonlethal quantification of cellular manganese. *J Biol Chem* **295**, 3875–3890 (2020).

46. Kaufman, R. J., Swaroop, M. & Murtha-Riel, P. Depletion of manganese within the secretory pathway inhibits O-linked glycosylation in mammalian cells. *Biochemistry* **33**, 9813–9819 (1994).

47. Masuda, M., Braun-Sommargren, M., Crooks, D. & Smith, D. R. Golgi phosphoprotein 4 (GPP130) is a sensitive and selective cellular target of manganese exposure. *Synapse* **67**, 205–215 (2013).

48. Mukhopadhyay, S. & Linstedt, A. D. Identification of a gain-of-function mutation in a Golgi P-type ATPase that enhances Mn2+ efflux and protects against toxicity. *Proc Natl Acad Sci U S A* **108**, 858–863 (2011).

49. Bowman, A. B. & Aschner, M. Considerations on manganese (Mn) treatments for in vitro studies. *Neurotoxicology* **41**, 141–142 (2014).

50. Van Baelen, K., Vanoevelen, J., Missiaen, L., Raeymaekers, L. & Wuytack, F. The Golgi PMR1 P-type ATPase of Caenorhabditis elegans. Identification of the gene and demonstration of calcium and manganese transport. *J Biol Chem* **276**, 10683–10691 (2001).

Figure Legends

Figure1. TMEM165 and SPCA1 expression in SPCA1 and TMEM165 KO cells, respectively.

A. Subcellular localization and abundance of TMEM165 and GM130 in HeLa control and SPCA1 KO cells. **B.** Expression of TMEM165 and SPCA1 in HeLa control cells versus SPCA1 KO cells. Total cell lysates were prepared, subjected to SDS–PAGE and Immunoblotted with the indicated antibodies. **C.** Expression and gel mobility of LAMP2 in HeLa control cells versus SPCA1 KO cells. **D.** Subcellular localization and abundance of TMEM165 and SPCA1 in HeLa control and TMEM165 KO cells. **E.** Expression of TMEM165 and SPCA1 in HeLa control cells versus TMEM165 KO cells. Total cell lysates were prepared, subjected to SDS–PAGE and Immunoblotted with the indicated antibodies. **F.** Expression and gel mobility of LAMP2 in HeLa control cells versus TMEM165 KO cells.

Figure 2. Golgi glycosylation defects in TMEM165 KO cells arise from a lack of Manganese in membrane bound organelles. Comparison of the steady state Mn contents in cytosol and membrane bound organelles in control, SPCA1 and TMEM165 KO HeLa cells, without and with 1μM MnCl2 supplementation.

A. Cytosol and membrane-bound organelle Mn contents in control, SPCA1 KO and TMEM165 KO HeLa cells without and with 1 μM Mn supplementation. Cells were permeabilized with digitonin, as described in Material and Methods section, to release the Mn cytosolic solutes while leaving the intracellular compartments intact. The graphs show the quantification of Mn contents of the three cell lines, supplemented or not with 1 μM Mn for 16h, within their cytosol (Cytosol – left panel) and membrane-bound organelles (Organelles – right panel) using quantification by inductively-coupled plasma mass spectrometry (ICP-MS), as described in Material and Methods section. Data are means ± standard deviation (SD) (n = 3). Statistical significance was determined by one-way ANOVA with multiple comparisons and is denoted

by the following: *, $p < 0.05$; **, $p < 0.01$; ***, $p < 0.001$. **B**. Expression of LAMP2, used as a glycosylation reporter, in TMEM165 KO HeLa cells without and with 1 μM Mn supplementation for 16 h. Western-blot and immunostaining of LAMP2 were performed as described in Material and Methods section. The vertical bars indicate the electrophoretic migration distances corresponding to the fully- (Fully-glyc.) and under- (Under-glyc.) glycosylated forms of LAMP2.

Figure 3. TMEM165 and SPCA1 are crucial in regulating cellular Mn homeostasis. Effects of MnCl2 supplementation up to 50 μM on the cytosol versus organelles steady state Mn contents of HeLa cells deficient or not in SPCA1 and/or TMEM165.

Cells were permeabilized with digitonin, as described in Material and Methods section, to release the Mn cytosolic solutes while leaving the intracellular compartments intact. The graphs show the quantification of Mn contents in the of the three cell lines, supplemented or not with different increasing MnCl2 concentrations (1, 2.5, 5, 25 and 50 μM) for 16 h, within their cytosol (Cytosol – left panel) and membrane-bound organelles (Organelles – right panel) using ICP-MS, as described in Material and Methods section. Data are means ± SD (n = 3). Statistical significance was determined by one-way ANOVA with multiple comparisons and is denoted by the following: *, $p < 0.05$; **, $p < 0.01$; ***, $p < 0.001$.

Figure 4. Cellular Mn homeostasis maintenance in control cells requires the presence of TMEM165. Impacts of high MnCl2 supplementation on the cytosol versus organelles steady state Mn contents of control, SPCA1 KO and TMEM165 KO HeLa cells.

A. Cytosol and membrane-bound organelle Mn contents in control, SPCA1 KO and TMEM165 KO HeLa cells supplemented or not with 100, 200 and 400 μM MnCl2. Cells were permeabilized with digitonin, as described in Material and Methods section, to release the Mn cytosolic solutes while leaving the intracellular compartments intact. The graphs show the quantification of Mn contents of the three cell lines, supplemented or not with different Mn

concentrations for 16 h, within their cytosol (Cytosol – left panel) and membrane-bound organelles (Organelles – right panel) using ICP-MS, as described in Material and Methods section. Data are means ± SD (n = 3). Statistical significance was determined by one-way ANOVA with multiple comparisons and is denoted by the following: *, $p < 0.05$; **, $p < 0.01$; ***, $p < 0.001$. **B.** TMEM165 stability in control HeLa cells supplemented or not with 100, 200 and 400 µM MnCl2. The Western-blot shows the presence and electrophoretic migration pattern of TMEM165 within control HeLa cells supplemented or not with MnCl2 for 16h, as described in Material and Methods section. TMEM165 KO HeLa cells submitted to the same conditions are used as TMEM165 protein expression controls. The vertical bars indicate the increasing presence of TMEM165 degradation forms upon Mn supplementation of HeLa cells from 200 to 400 µM MnCl2. The graph on the right depicts the quantification of relative TMEM165 protein expression in control cells upon MnCl2 treatment. Data are means ± SD (n = 3).

Figure 5. Mn detoxification is altered in SPCA1 KO and TMEM165 KO HeLa cells.

Control Hela cells were incubated with 400µM MnCl2 for 16h, SPCA1 and TMEM165 KO cells with 100µM MnCl2 for 16h. Cells were then washed and incubated for 3 and 6h in a MnCl2 –free medium. The graphs show the quantification of the cytosol versus organelles steady state Mn contents of control, SPCA1 KO and TMEM165 KO HeLa cells using ICP-MS. Data are means ± SD (n = 3). Statistical significance was determined by one-way ANOVA with multiple comparisons and is denoted by the following: *, $p < 0.05$; **, $p < 0.01$; ***, $p < 0.001$.

Figure 6. Cellular model for TMEM165 and SPCA1's functioning.

A. In absence of TMEM165, the cytosolic Mn is not efficiently transported into the Golgi apparatus (GA). As most of the Golgi glycosyltransferases require Mn as cofactor, general Golgi glycosylation defects are observed. **B.** Exogenous Mn supplementation in TMEM165

KO cells rescues the Golgi glycosylation defects. In absence of TMEM165, the cytosolic Mn accumulation is pumped by thapsigargin (TG)-sensitive pumps, likely ER Serca pumps. The redistribution of Mn to the Golgi allows the functioning of glycosylation enzymes. **C.** Under moderate exogenous Mn concentrations (0-200 μM), TMEM165 would play a crucial role in both detoxifying accumulating cytosolic Mn and bringing Mn inside the Golgi lumen to sustain the activities of glycosyltransferases. This would allow the function of SPCA1 in Ca pumping. **D.** Under exogenous Mn concentrations higher than 200μM, TMEM165 would be degraded to "turn on" SPCA1 in the Mn detoxification pathway.

Supplementary Figure 1: Stability of SPCA1 depends on TMEM165 expression in TMEM165 KO cells.

Expression of SPCA1 in TMEM165 KO HeLa cells after transient expression of wt-TMEM165 by immunofluorescence.

Supplementary Figure 2: Schematic workflow of the developed sample preparation for cytosolic and membrane-bound organelles Mn quantification via ICP-MS analysis.

A. Cells before treatment with digitonin. **B**. Permeabilization of the plasma membranes with digitonin. The cytosolic fraction is collected. **C**. Lysis of the cells and sonication of the lysate. The membrane-bound organelles fraction is collected.

Supplementary Figure 3: Comparison of the steady state Mn contents in cytosol and membrane bound organelles in control and SPCA1 KO HAP1 cells.

Cytosol and membrane-bound organelle Mn contents in control, SPCA1 KO HAP1 cells. Cells were permeabilized with digitonin, as described in Material and Methods section, to release the Mn cytosolic solutes while leaving the intracellular compartments intact. The graphs show the quantification of Mn contents of control and SPCA1 KO HAP1 cells within their cytosol (Cytosol – left panel) and membrane-bound organelles (Organelles – right panel) using ICP-

MS, as described in Material and Methods section. Data are means ± standard deviation (SD) (n = 3).

Supplementary Figure 4: Statistical significance of the effects of MnCl2 supplementation up to 50 µM on the cytosol versus organelles steady state Mn contents of HeLa cells deficient or not in SPCA1 and/or TMEM165. The graphs show the quantification of Mn contents in the of the three cell lines, supplemented or not with different increasing MnCl2 concentrations (1, 2.5, 5, 25 and 50 µM) for 16 h, within their cytosol (Cytosol – left panel) and membrane-bound organelles (Organelles – right panel) using ICP-MS, as described in Material and Methods section. Data are means ± SD (n = 3). Statistical significance was determined wherever it was possible by one-way ANOVA with multiple comparisons and is denoted by the following: *, $p < 0.05$; **, $p < 0.01$; ***, $p < 0.001$.

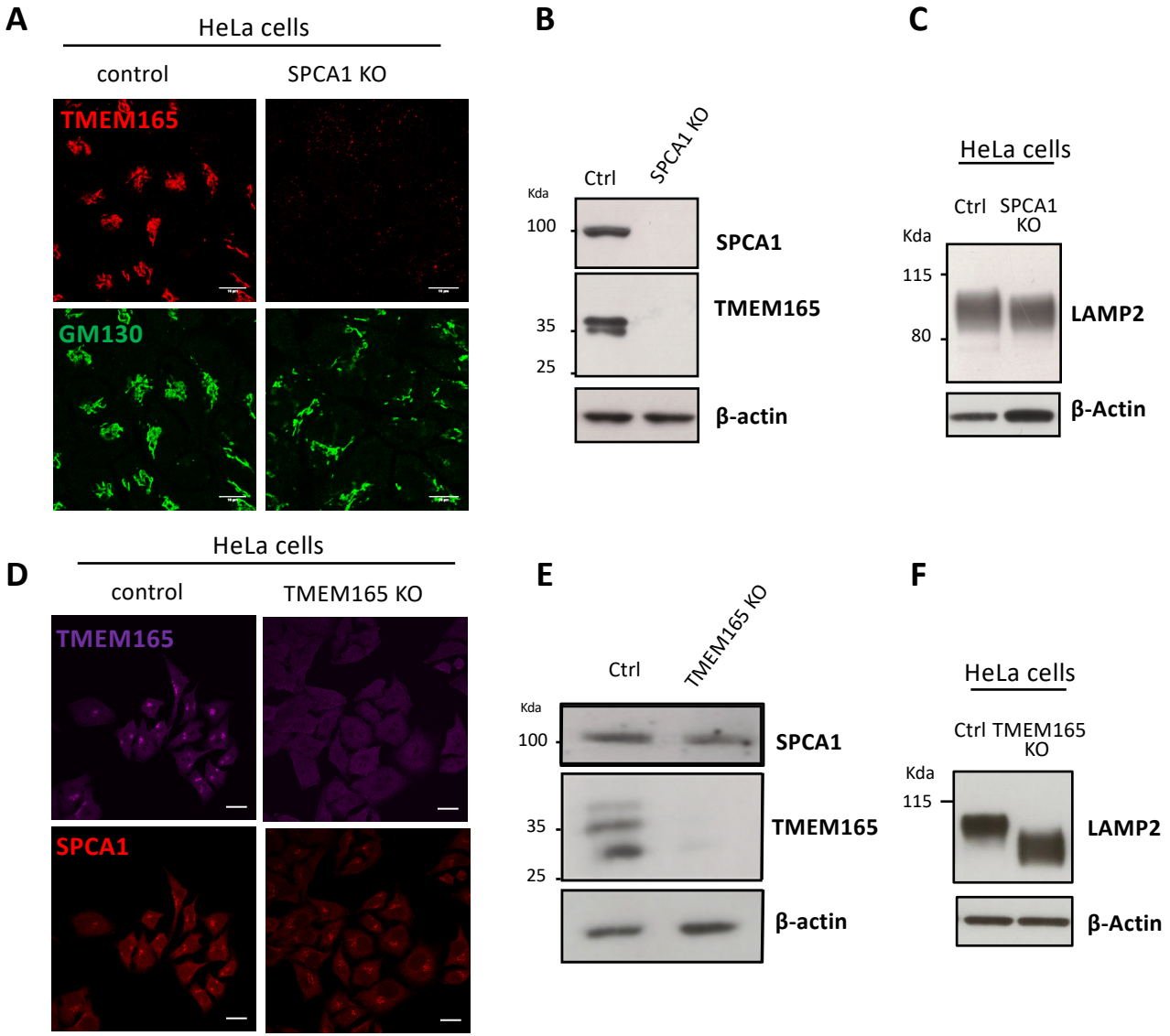
A
HeLa cells
control
SPCA1 KO
TMEM165
GM130
B
Ctrl
SPCA1 KO
Kda
100
35
25
SPCA1
TMEM165
β-actin
C
HeLa cells
Ctrl
SPCA1 KO
Kda
115
80
LAMP2
β-Actin
D
HeLa cells
control
TMEM165 KO
TMEM165
SPCA1
E
Ctrl
TMEM165 KO
Kda
100
35
25
SPCA1
TMEM165
β-actin
F
HeLa cells
Ctrl
TMEM165 KO
Kda
115
LAMP2
β-Actin

Figure 1

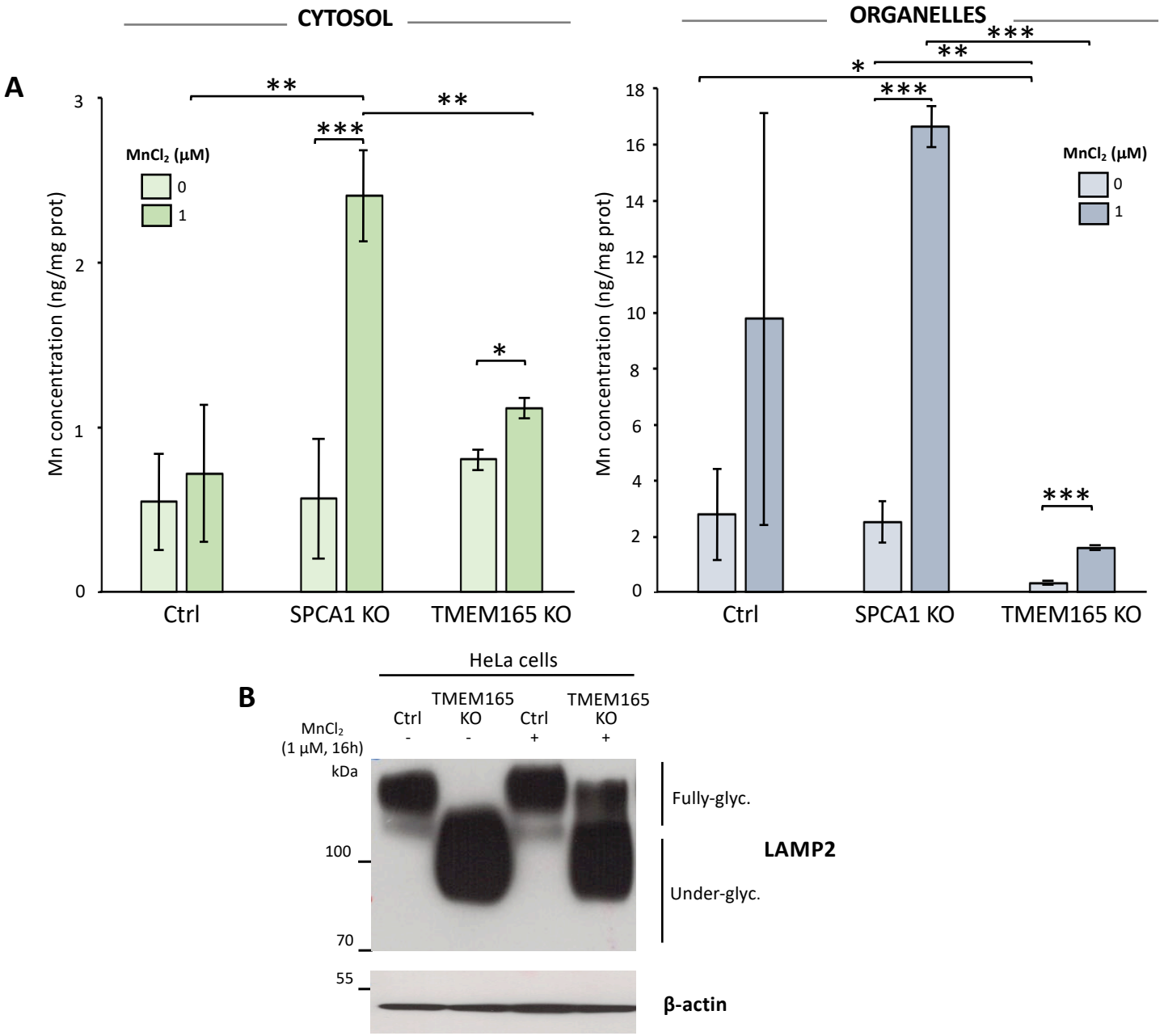
A
CYTOSOL
ORGANELLES
Mn concentration (ng/mg prot)
MnCl2 (µM)
0
1
Ctrl
SPCA1 KO
TMEM165 KO
B
HeLa cells
Ctrl
TMEM165 KO
Ctrl
TMEM165 KO
MnCl2 (1 µM, 16h)
kDa
100
70
55
Fully-glyc.
Under-glyc.
LAMP2
β-actin

Figure 2

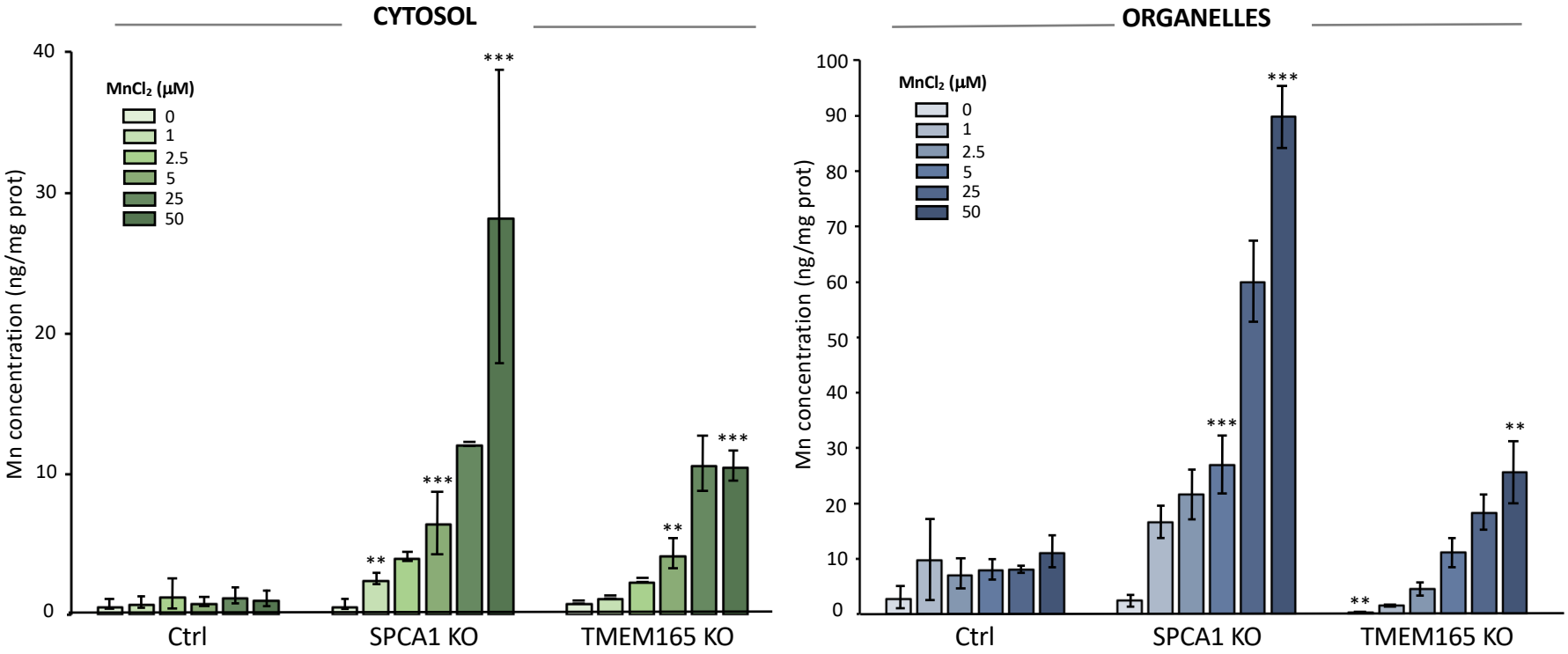
CYTOSOL
ORGANELLES
MnCl₂ (µM)
0
1
2.5
5
25
50
Mn concentration (ng/mg prot)
Ctrl
SPCA1 KO
TMEM165 KO
***
**

Figure 3

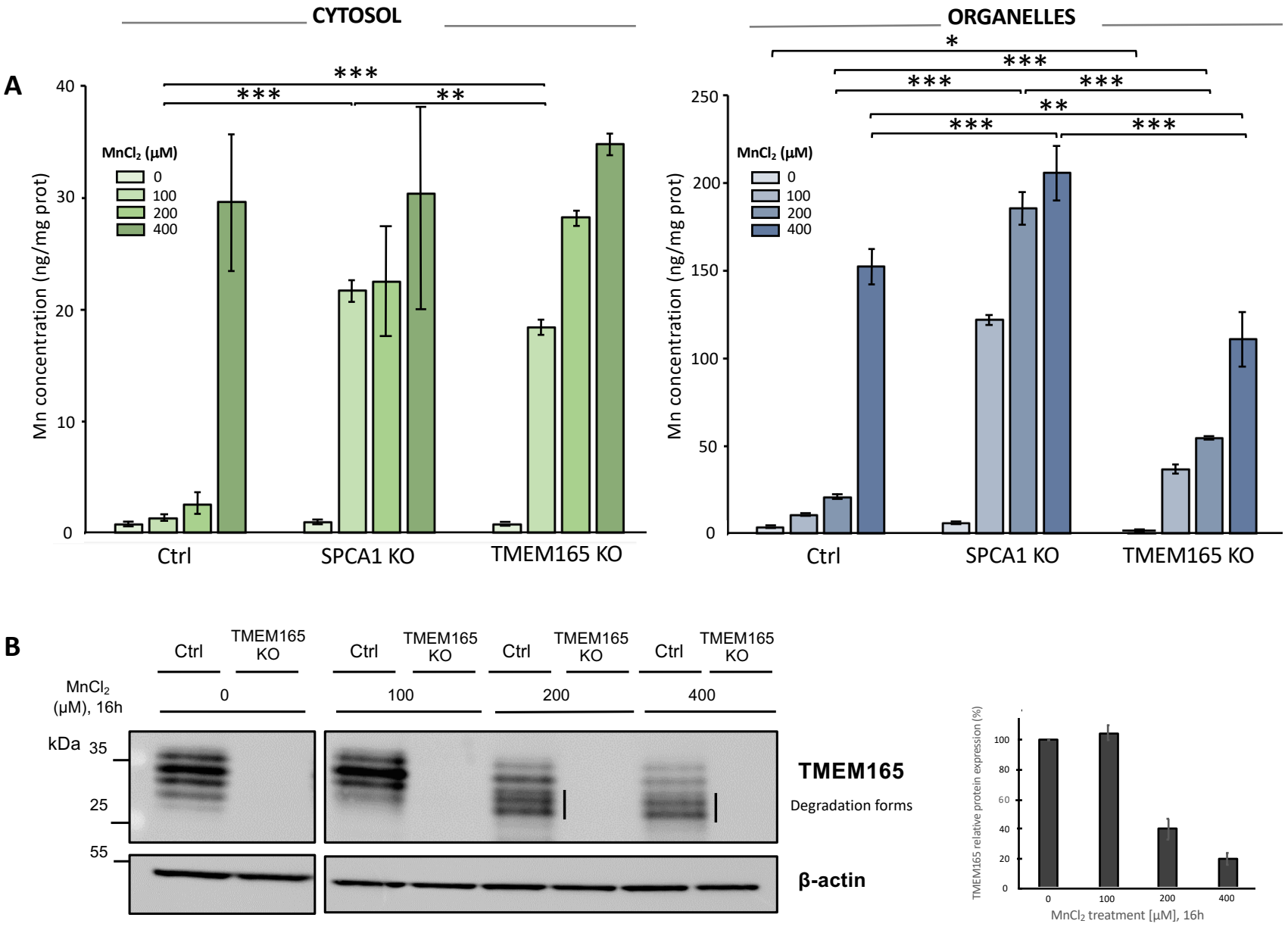
A
CYTOSOL
ORGANELLES
Mn concentration (ng/mg prot)
MnCl2 (µM)
0
100
200
400
Ctrl
SPCA1 KO
TMEM165 KO
B
Ctrl
TMEM165 KO
MnCl2 (µM), 16h
kDa
35
25
55
TMEM165
Degradation forms
β-actin
TMEM165 relative protein expression (%)
MnCl2 treatment [µM], 16h

Figure 4

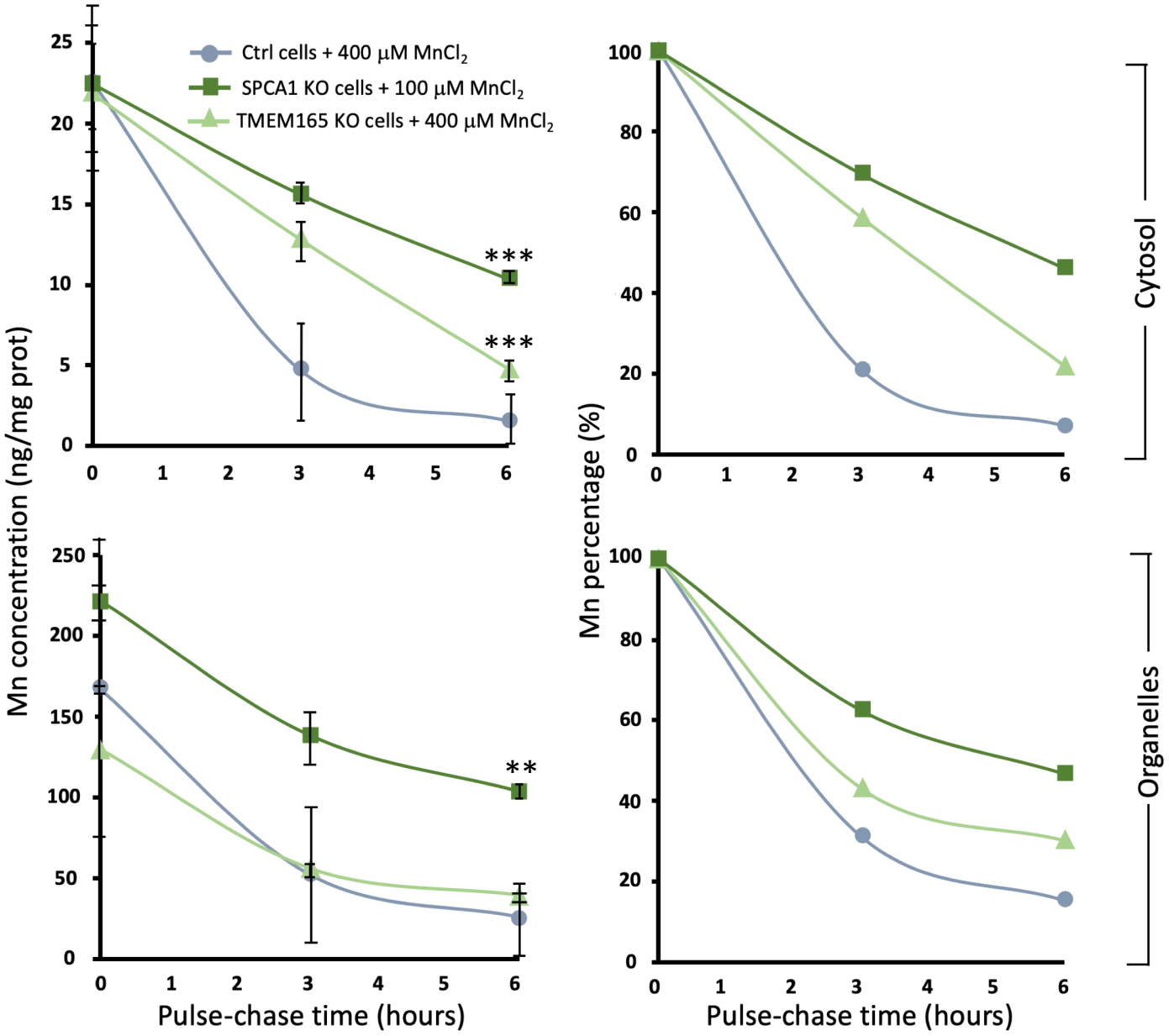
Ctrl cells + 400 µM MnCl2
SPCA1 KO cells + 100 µM MnCl2
TMEM165 KO cells + 400 µM MnCl2
Mn concentration (ng/mg prot)
Mn percentage (%)
Pulse-chase time (hours)
Pulse-chase time (hours)
***
***
**
Cytosol
Organelles

Figure 5

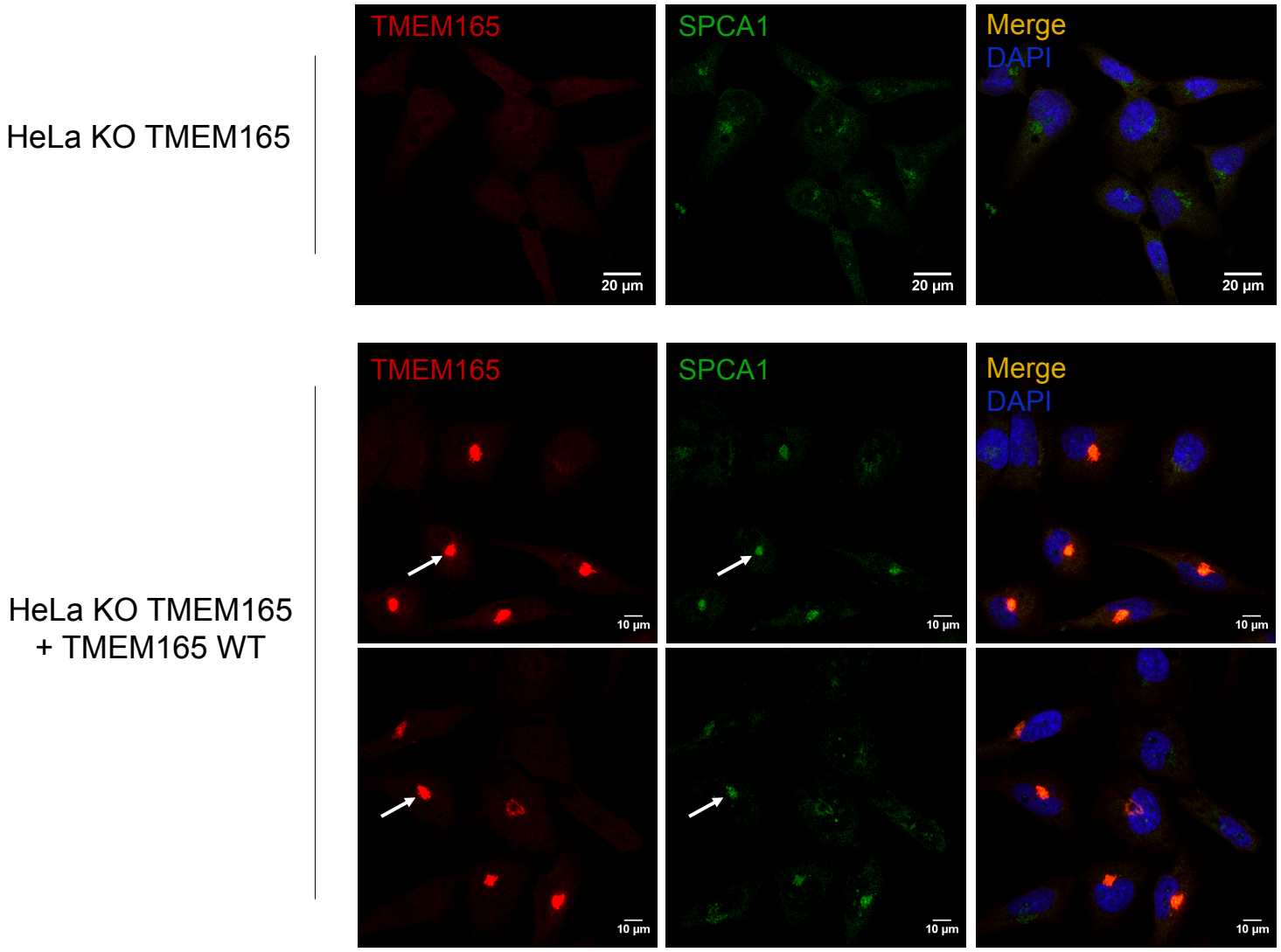

Supp. Figure 1

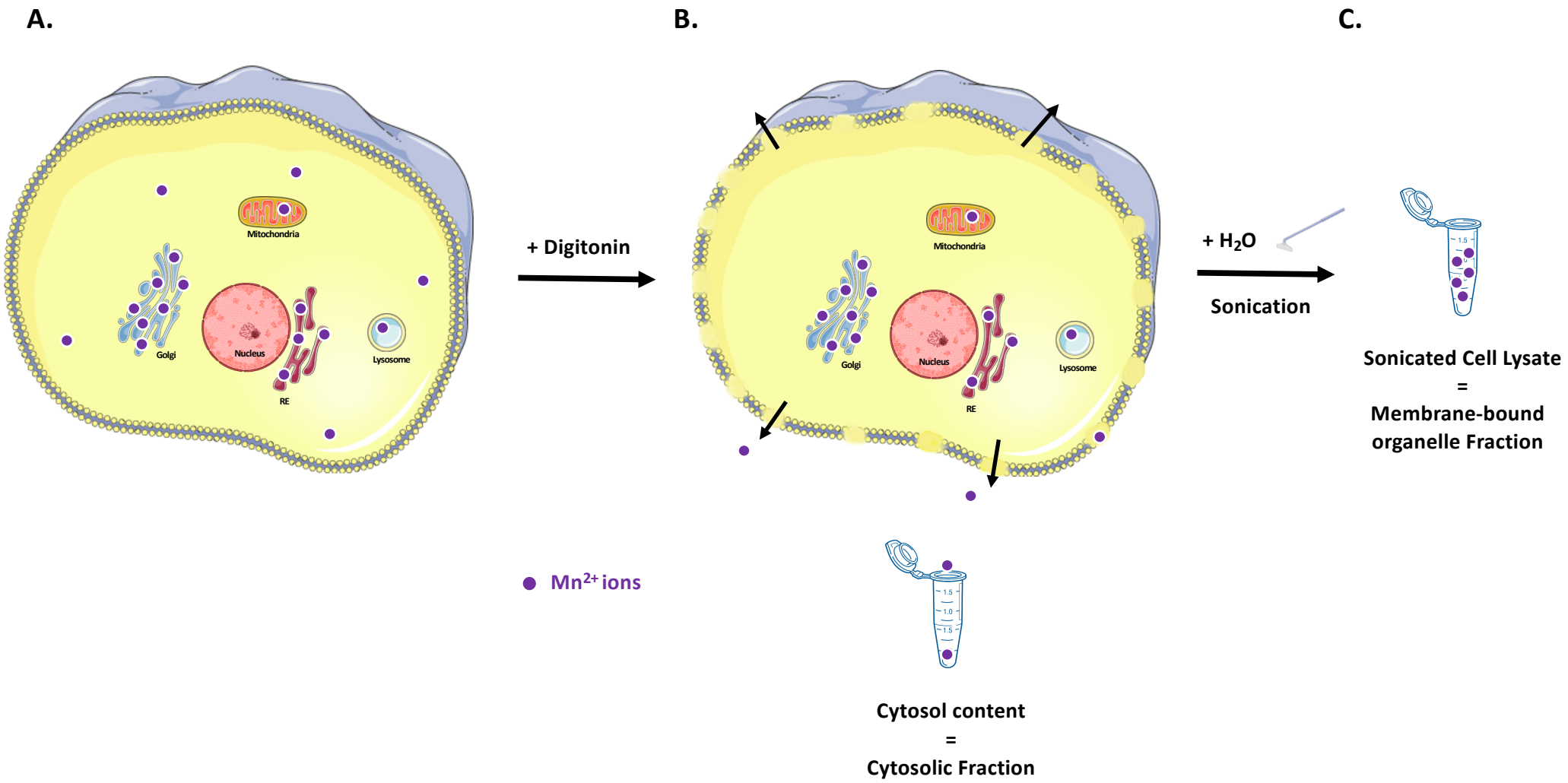

Supp. Figure 2

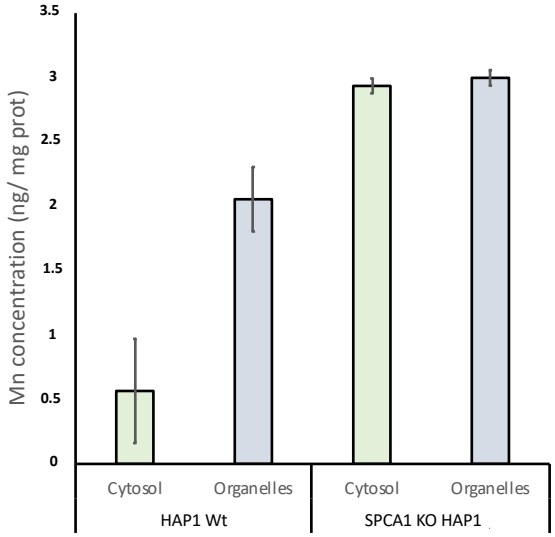

Supp. Figure 3

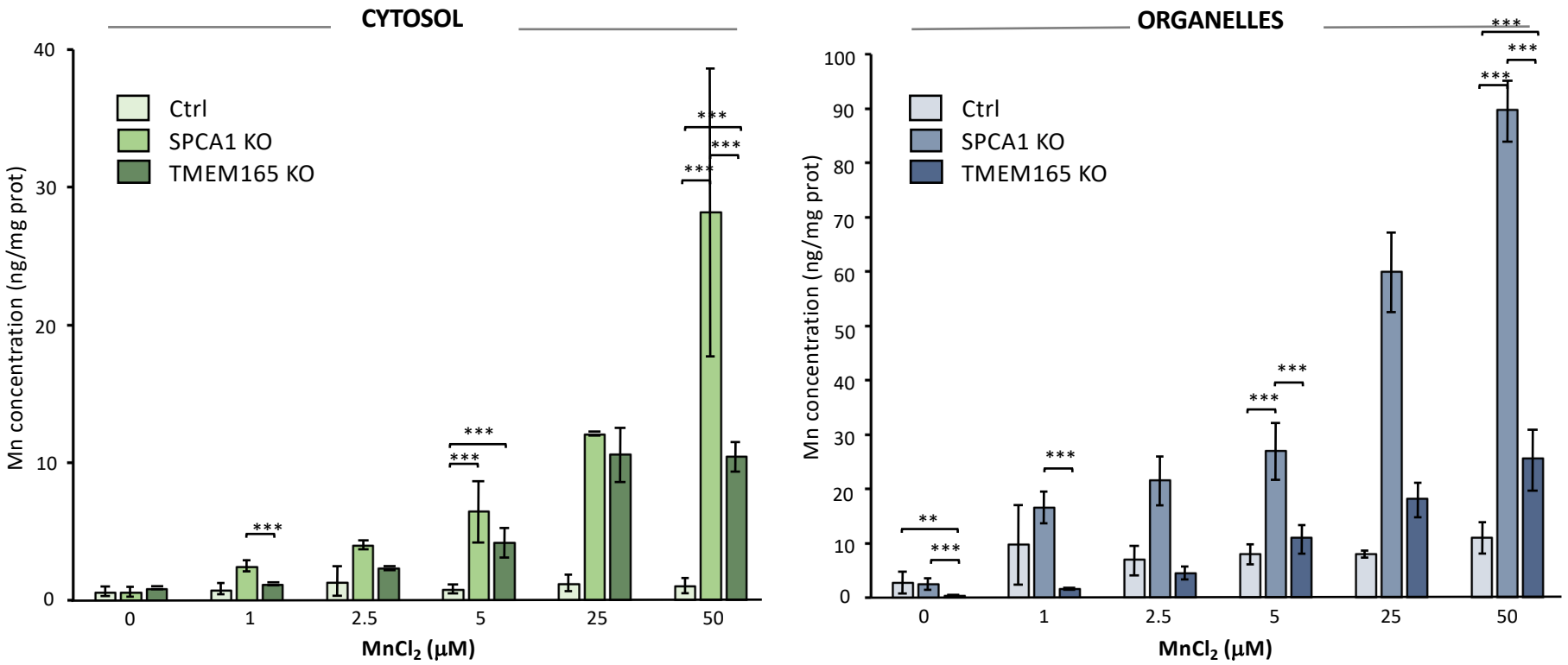

Supp. Figure 4